Soft Matter

PAPER

View Article Online
View Journal | View Issue

Cite this: *Soft Matter*, 2025, 21, 8692

Superior affinity of ubiquicidin peptide united with *ortho*-borylated acetophenone to an amine-containing model bacterial membrane

Sonam Raghav,[a] Bibekananda Pati,[b] Nancy Jaglan,[a] Archana Mukherjee,[cd] Veerendra K. Sharma, *[de] Anupam Bandyopadhyay *[b] and Sajal K. Ghosh *[a]

Antimicrobial peptides (AMPs) have been considered as potential agents to combat bacterial resistance to conventional antibiotics. It has been shown that modifying the cationic peptides with 2-acetylphenylboronic acid (2-APBA) improves the binding efficacy with these resistant bacterial membranes *via* the formation of a covalent iminoboronate bond with lipids, such as 1,2-dioleoyl-*sn*-*glycero*-3-[phospho-*rac*-(3-lysyl(1-*glycerol*))] (Lys PG). In the present study, the cationic peptide UBI (29–41) is modified with 2-APBA at the C-terminus to investigate its affinity to membranes of such lipids. The surface pressure–area isotherm, dilation rheology and atomic force microscopy (AFM) studies are performed on the monolayers formed at the air–water interface by the cationic lipid Lys PG and 1,2-distearoyl-*sn*-*glycero*-3-ethylphosphocholine (DSEPC). The modified UBI-2-APBA substantially enhances its membrane affinity compared to the unmodified UBI (29–41). This observation is consistent with covalent bond formation *via* iminoboronate linkages. However, the cationic lipid Lys PG exhibits an insertion of UBI-2-APBA into the lipid film, whereas DSEPC shows only an adsorption of the peptide. Interestingly, the affinity of both the peptides to zwitterionic lipid 1,2-distearoyl-*sn*-*glycero*-3-phosphoethanolamine (DSPE) is found to be similar. Therefore, the findings here indicate the potential of 2-APBA functionalization of peptides as a powerful strategy to selectively target bacterial membranes.

Received 6th July 2025,
Accepted 21st October 2025

DOI: 10.1039/d5sm00692a

rsc.li/soft-matter-journal

1. Introduction

Antibiotic resistance (AMR) has emerged as one of the most critical threats to global public health, and is projected to cause 39 million indirect deaths in the next 25 years.[1] AMR, driven largely by the inappropriate and excessive use of antibiotics, is now recognized as an accelerating global health crisis.[2] 'Superbugs' have emerged, such as *Mycobacterium tuberculosis*, vancomycin-resistant *Enterococcus* (VRE), and methicillin-resistant *Staphylococcus aureus* (MRSA), all of which can cause untreatable infections.[3–5] The escalation of such global threats highlights the urgent need for novel antimicrobial agents. Antimicrobial peptides (AMPs) have emerged as potent alternatives to conventional antibiotics due to their broad spectrum of activity and rapid bactericidal effects. Their ability to penetrate tissues and selectively target bacterial membranes makes them highly attractive for therapeutic development.[6,7]

Among bacterial pathogens, *Staphylococcus aureus* (*S. aureus*) remains one of the most well-known causes of hospital and community acquired infections.[8] It appears to introduce a critical mechanism of resistance to cationic AMPs *via* the modification of the membrane lipids, particularly the saturated species, such as dipalmitoyl phosphatidylglycerol (DPPG) into lysyl-phosphatidylglycerol (Lys PG) (Fig. 1a).[9] This process occurring after PG biosynthesis is catalysed by the bifunctional membrane protein MprF, which transfers an L-lysine moiety from lysyl-tRNA to PG and translocates the resulting Lys PG to the outer leaflet of the cytoplasmic membrane.[10] This modification alters the net charge of the lipid from negative to positive, repelling the cationic AMP and reducing its effectiveness in membrane disruption.[9] Achieving selective and strong interactions of a cationic AMP to *S. aureus* membrane requires strategies that account for these complex biochemical adaptations.

Ubiquicidin (UBI), a human colon mucosa antimicrobial protein, is broadly conserved in all eukaryotic organisms,

[a] *Department of Physics, School of Natural Sciences, Shiv Nadar Institution of Eminence, NH 91, Tehsil Dadri, G.B. Nagar, Uttar Pradesh 201314, India. E-mail: sajal.ghosh@snu.edu.in*
[b] *Biomimetic Peptide Engineering Laboratory, Department of Chemistry, Indian Institute of Technology, Ropar, Rupnagar, Punjab 140001, India. E-mail: anupamba@iitrpr.ac.in*
[c] *Radiopharmaceuticals Division, Bhabha Atomic Research Centre, Mumbai 400085, India*
[d] *Homi Bhabha National Institute, Mumbai 400094, India*
[e] *Solid State Physics Division, Bhabha Atomic Research Centre, Mumbai 400085, India. E-mail: sharmavk@barc.gov.in*

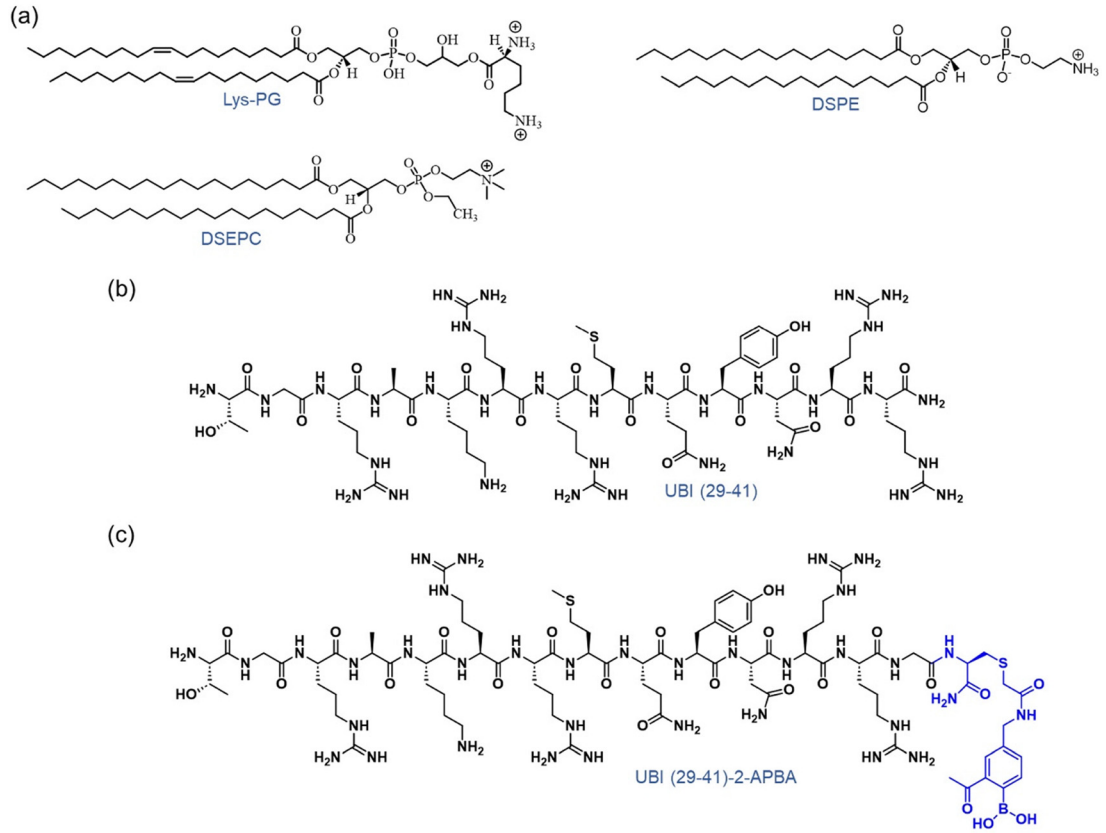

Fig. 1 Chemical structure of (a) lipids Lys PG, DSEPC and DSPE, and (b) antimicrobial peptide ubiquicidin (29–41), and (c) ubiquicidin (29–41)-2-APBA.

suggesting that it plays a substantial role in innate defence.[11] The cationic UBI (29–41) peptide, murine ubiquicidin peptide, has high selectivity for bacterial membranes with a high proportion of positive residues—five arginine's and one lysine—for electrostatic binding to negatively charged bacterial surfaces (Fig. 1b).[7,12] However, this cationic peptide may be inactive in targeting an antimicrobial-resistant bacterium with a higher quantity of positively charged lipids, like Lys PG, in its membrane. Therefore, alternative approaches, such as chemical modification of peptides, are necessary to develop AMPs with better interaction with bacterial plasma membranes. *ortho*-Borylated acetophenone or 2-acetylphenylboronic (2-APBA) acid that forms a dynamic covalent bond with amine *via* iminoboronate formation has emerged as an attractive covalent probe to modulate AMP's binding ability to *S. aureus* with altered Lys PG distribution on the outer membrane.[13–16] Targeting amines through covalent linkage on amino acylated lipids (Lys PG) offers an innovative approach to combating the challenges of interacting with the cationic membrane.

Recent work has indicated that conjugation of 2-acetylphenylboronic acid (2-APBA) to ubiquicidin (UBI) derivatives improves bacterial uptake and increases *in vivo* imaging retention compared with unmodified UBI.[14,15] In some cases, these conjugates were able to kill bacteria or disrupt their membrane, most likely due to the reversible iminoboronate linkage allowing stronger attachment to the membrane. This highlights how combining electrostatic interaction with covalent bonding can improve antimicrobial activity.

Contingent on the progress of iminoboronate chemistry-based lipid recognition, we noticed a research gap for in-depth biophysical investigation of amine presenting membrane recognition with 2-APBA-modified AMPs. In addition, the physicochemical properties of the membrane presenting Lys PG with other lipids and their comparative interaction with 2-APBA-edited AMPs are less exploited. In the present work, we address this gap using complimentary approaches. Specifically, we quantify peptide–lipid interactions through surface pressure–area isotherms, dilation rheology and AFM, which probe in plane viscoelastic properties and visualize morphological changes in the monolayer system. In addition, we monitor the kinetics of surface pressure changes following peptide injection to resolve the time-dependent insertion of UBI and its covalent analogue UBI-2-APBA into the Lys PG monolayers. Together, these methods provide a comprehensive picture of how the pressure, packing and time-dependent process shape peptide insertion and membrane perturbation. Note that the biomimetic lipid monolayer composed of cationic Lys PG and DSEPC, along with zwitterionic DSPE lipids, was engineered to simulate a single leaflet of a bacterial membrane to duplicate its central composition.

2. Materials and methods

2.1. Materials

Positively charged phospholipids 1,2-dioleoyl-*sn-glycero*-3-[phospho-*rac*-(3-lysyl(1-*glycerol*))] (chloride salt) (Lys PG) and

1,2-distearoyl-*sn-glycero*-3-ethylphosphocholine (chloride salt) (DSEPC) and zwitterionic phospholipids 1,2-distearoyl-*sn-glycero*-3-phosphoethanolamine (DSPE) were purchased from Avanti Polar Lipids (Alabaster, USA) in powder form, and were used without further purification. The spectroscopy-grade solvents chloroform and methanol were also purchased from Sigma Aldrich (USA). UBI (29–41) with sequence TGRAKRRMQYNRR was procured from ABI Scientific (Sterling, US), whereas 2-APBA probe was synthesized following the processes described elsewhere.[17] Furthermore, the probe was conjugated with UBI (29–41)–G–C peptide. The details of the synthesis method are provided in Section S1 of the supplementary information (SI). The purity of the peptides was greater than 90%.

2.2. Methods

2.2.1. Surface pressure–area isotherms. A medium-sized Langmuir–Blodgett (LB) trough (trough top inner dimensions $364 \times 75 \times 4$ mm^3) KSV NIMA, Biolin Scientific) was equipped with a platinum Wilhelmy balance and two Delrin barriers, which were used to characterize the surface pressure–area isotherms of the lipids. For isotherm measurements, deionized millipore water (resistivity 18.2 MΩ cm) was used as the subphase. Lipids were dissolved in chloroform, while the peptide was dissolved in methanol. These two solutions were then combined at a volume ratio 3 : 1 (chloroform : methanol) to ensure homogeneous mixing. The final stock solution had a mass concentration of 0.5 mg mL^{-1}, corresponding to molar concentrations of 0.51 mM for pure Lys PG, 0.58 mM for DSEPC, and 0.67 mM for DSPE. The molar percentage of AMP in the mixed system was calculated using the expression, $\chi_{AMP} = \frac{\frac{X}{M_{AMP}}}{\frac{X}{M_{AMP}} + \frac{Y}{M_{Lipid}}} \times 100\%$ where, χ_{AMP} is the molar percentage of AMP, X and Y are the measured masses, and M_{AMP} and M_{Lipid} represent the molecular masses of AMP and lipid, respectively.[18] For the formation of a monolayer, 40 μL of pure lipid solution was uniformly spread at the air–water interface using a glass Hamilton micro syringe. The amount of lipid molecules was calculated from this volume and was kept constant in all experiments. In peptide–lipid systems, the amount of peptide to be included was measured to obtain a specific molar ratio (*e.g.* 80 : 20 mol%), keeping the same number of lipid molecules. Hence, any change noticed in the isotherms is due to peptide–lipid interaction only. The trough was then left undisturbed for 45 minutes to allow the volatile solvent to evaporate. The water temperature was maintained at 22 ± 1 °C using a water bath circulator (Equitron, India). Subsequently, the Delrin barriers were symmetrically compressed at a constant rate of 4 mm min^{-1}. The surface pressure was recorded as a function of the area per molecule, constructing the surface pressure–area isotherm. To avoid any contamination, before each measurement, the LB trough and platinum Wilhelmy plate were thoroughly cleaned with ethanol and deionized water to remove any organic traces.

2.2.2. In-plane rheology. Dilation rheology experiments were conducted using the same Langmuir–Blodgett trough as mentioned above. A target surface pressure of 25 mN m^{-1} was reached by slowly compressing the molecular layer at a rate of 2 mm min^{-1}. The barriers of the trough were made sinusoidally oscillated at a specific frequency. An area amplitude of 0.5% was calculated using $\frac{\Delta A}{A} \times 100\%$, where A is the mean molecular area at the target surface pressure, and ΔA is the change in A. Because of the viscoelastic nature of the film, there is a phase lag ϕ between stress and strain. This phase difference (ϕ) was used to calculate the viscoelastic parameters, storage modulus, $E' = \frac{\pi_0}{A_0}\cos\phi$ and loss modulus, $E'' = \frac{\pi_0}{A_0}\sin\phi$, where π_0 and A_0 are the stress and strain amplitudes, respectively.[19–22] Measurements were performed over a frequency range of 10–100 mHz with increment of 10 mHz. More details of the data and analysis are available in Section S2 of the SI.

2.2.3. Surface potential. The surface potential of the molecular film at the air–water interface was measured simultaneously with the isotherm data using the KSV NIMA surface potential sensor (SPOT) equipped with the LB trough. This technique employs the vibrating plate capacitor method, also known as the vibrating plate Kelvin method. This method measured the potential difference between a counter electrode submerged in the subphase (beneath the molecular film) and a vibrating plate positioned in the air, approximately 4 mm above the water surface.

The surface potential of the lipid layer was measured using the air–water interface as the reference potential, which was zeroed prior to spreading the lipid molecules. Immediately after spreading the lipid molecules on the water surface, a noticeable fluctuation in potential was observed. To allow the system to stabilize and reach an equilibrated value, it was left undisturbed for approximately 45 minutes.

2.2.4. Time dependent surface pressure. For measuring the surface pressure, a Petri dish (diameter 5 cm, height 1.2 cm) was filled with 15 mL of water and a Wilhelmy plate microbalance was used to measure the surface pressure. The lipid solution of 0.5 mg ml^{-1} in chloroform was spread on the water surface using a Hamilton syringe until the surface pressure reached a value of 20 mN m^{-1}, which was then left to equilibrate for ∼30 min. Then, 91 μl of aqueous solution of peptide with a concentration of 0.5 mg ml^{-1} was injected into the subphase of the equilibrated lipid layer. This event was monitored as a function of time. Because of the fixed diameter of the Petri dish, the area of the water surface was fixed during the assembly of the peptide around the lipid film. All measurements were conducted at the same temperature of 22 ± 1 °C.

2.2.5. Atomic force microscopy (AFM). AFM imaging of phospholipid monolayers was performed by dip coating them on a silicon substrate (1.5×1 cm^2; n-type, ⟨100⟩ orientation, 500 μm thick; WaferPro). The substrates were cleaned following the RCA protocol described elsewhere.[23] Then they were UV-ozone treated at 50 °C for 30 min to make the surfaces hydrophilic. First a substrate was immersed in the subphase

of the Langmuir trough. Then a floating lipid layer was formed at the air–water interface following which the substrate was raised in the upstroke with a speed of 2 mm min^{-1} at a surface pressure of 30 mN m^{-1}.[24] This substrate coated with the lipid monolayer was vacuum dried (Metrex Scientific Instruments, India) at room temperature for about six hours and used for AFM (MFP-3D, Asylum Research, Santa Barbara, USA) imaging in intermittent contact mode.

3. Results and discussion

In this study, the interactions of ubiquicidin-derived peptide UBI (29–41) and its chemically modified variant UBI-2-APBA with a leaflet of model membranes were systematically investigated to gain insights into their potential as antimicrobial agents against resistant strains such as *S. aureus*. Specifically, the focus was on their interactions with positively charged lipids, particularly Lys PG, a major lipid component that causes AMP-resistance. To probe these interactions, surface pressure–area (π–A), and surface potential–area (ΔV–A) isotherms of the lipid monolayer were measured. Additionally, in-plane interfacial rheology was utilized to assess alterations in the viscoelastic behaviour of the lipid–peptide film at the air–water interface. For comparative evaluation, experiments were also conducted using cationic lipid 1,2-distearoyl-*sn-glycero*-3-ethylphosphocholine (DSEPC) and zwitterionic lipids 1,2-distearoyl-*sn-glycero*-3-phosphoethanolamine (DSPE). These DSEPC and DSPE lipid monolayers serve as controls to discern peptide selectivity and specificity.

3.1. Higher affinity of the modified peptide to cationic lipids

The pressure–area (π–A) isotherm technique is a crucial method for investigating the phase behaviour of monolayers of amphiphiles and studying the interactions of these molecules with others like cholesterol, drug molecules, proteins, and peptides. In a typical π–A isotherm, lipid molecules initially occupy a high mean molecular area (MMA) at the air–water interface, resulting in a gaseous (G) phase where molecular interactions are minimal and surface pressure is negligible. Upon compression, the molecules are drawn closer together, leading to increased intermolecular interactions and a rise in surface pressure. This transition from the gaseous (G) phase to the liquid expanded (LE) phase is marked by the onset of non-zero surface pressure, which occurs at an MMA, denoted "A_{max}" (arrow in Fig. 2(a)), the point where the molecules begin to interact. As compression continues, the monolayer progresses into the liquid-condensed (LC) phase, where molecules are closely packed, and surface pressure reaches a maximum value. The LC phase can sustain up to a critical "collapse pressure", beyond which the monolayer destabilizes, either forming multiple lipid layers or dissolving into the bulk subphase. In many cases of amphiphiles, the intermediate region between the LE and LC phases, characterized by a plateau in the isotherm, is considered a coexistence region, signifying a first-order phase transition between the two phases. The stability of the monolayer assembly is generally imparted by electrostatic, hydrophobic, hydrophilic, and van der Waals interactions, depending on the type of molecules involved. This study recorded all isotherms at a fixed water subphase temperature of 22 °C to analyse the molecular interactions.

The isotherms of pristine Lys PG lipid with 20 mol% of UBI (29–41) and its modified variant, UBI-2-APBA, are presented in Fig. 2(a). Such a simplified system is highly effective for gaining insights into the affinity of AMPs to membranes. Each isotherm is the average of at least three independent measurements. The errors presented in the extracted parameters are the standard deviation calculated from repeated measurements. A peptide concentration of 20 mol% relative to the lipids was selected, as this level is useful for investigating peptide–lipid interactions under such conditions where membrane perturbation becomes significant, producing noticeable effects on membrane assembly. Even though the quantity is physiologically high, such a high concentration has been used earlier in biophysical studies where the experimental techniques are not sensitive enough to perceive the changes at lower concentrations.[25] Pure UBI (29–41) and UBI-2-APBA, as cationic peptides, do not exhibit any isotherm as they lack the amphiphilic balance necessary for adsorption at the air–water interface (Fig. 2(a)). These cationic peptides have strong hydrophilic interactions with the surrounding water due to their charged residues, which prevent them from effectively partitioning at the interface. Additionally, their structural features may hinder the alteration of packing or orientation to assemble at the interface on their own.[26]

The isotherm of Lys PG exhibits an A_{max} of 183.5 $Å^2$, as shown in Fig. 2(b) and in Table 1. The lysine residue attached to the PG head results in a high cross-sectional area compared to other unsaturated lipids, leading to a higher value of A_{max}. The electrostatic repulsion among the charged head groups could also contribute to this high value. In the presence of UBI (29–41), the monolayer shifts to a slightly higher A_{max} of 187.3 $Å^2$, reflecting an interaction between the peptide and lipid molecules.[25] When UBI-2-APBA is incorporated into the monolayer, the A_{max} increases to 209.4 $Å^2$, indicating a stronger interaction (Fig. 2(b)). The presence of the modified moiety in UBI-2-APBA, which contains an additional 2-APBA group, likely enhances its interaction with the lipid layer. This increase can be attributed to the covalent interaction introduced by the iminoboronate linkage between the 2-APBA group and the Lys PG. A detailed study on such a linkage formation has been reported elsewhere.[13,14] In contrast, UBI (29–41), which is lacking in this functional group, exhibits relatively weaker interactions. Even though the lipid and the peptide both have a positive charge, which is supposed to cause a repulsion among the molecules, the functional group in UBI-2-APBA causes an effective attraction, demonstrating how specific moieties can significantly influence peptide–lipid interaction.

The limit area, A_{lim}, in an isotherm refers to the estimated area per molecule in the most tightly packed state, determined by extrapolating the linear portion of the isotherm to zero surface pressure, as demonstrated in Fig. 2(a). The limit area, A_{lim}, for Lys PG is found to be 141.75 $Å^2$. Upon the addition of UBI (29–41), A_{lim} increases to 146.5 $Å^2$, while the UBI-2-APBA results in a further increased value of 155.6 $Å^2$ (Fig. 2(c)). The

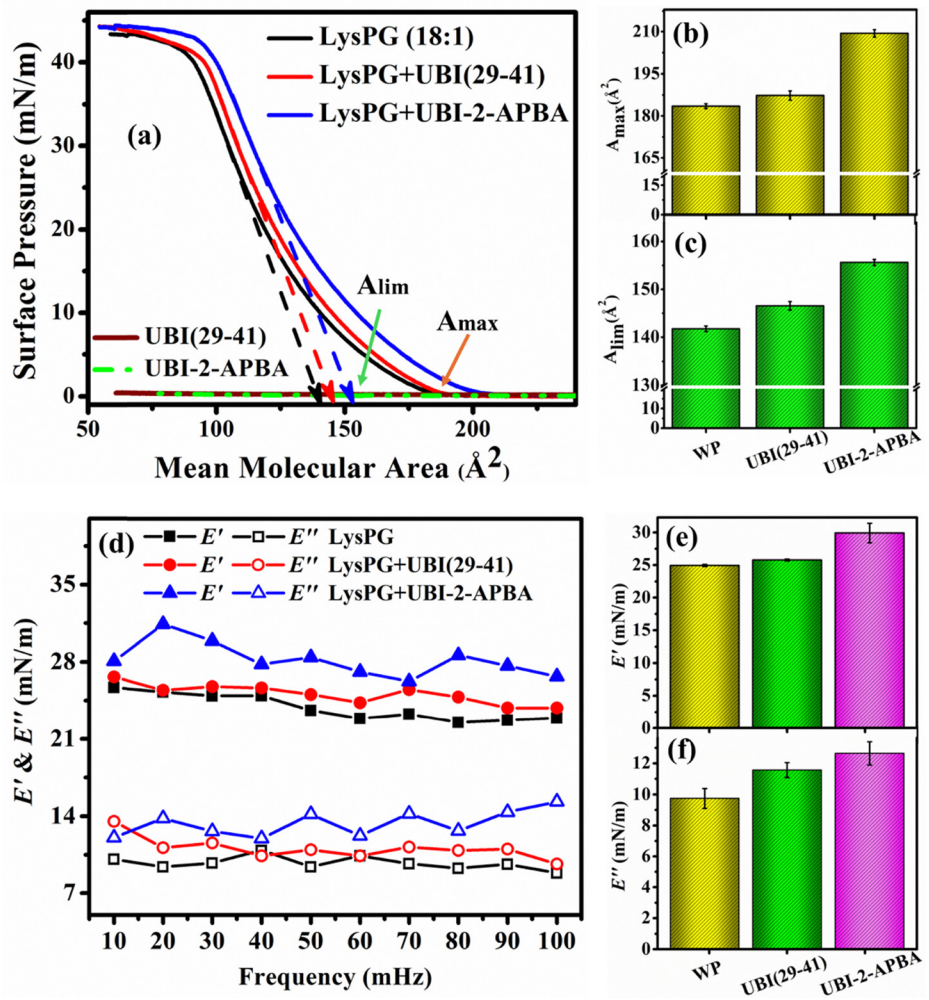

Fig. 2 (a) Surface pressure (π)–area (A) isotherms of the Lys PG monolayer at the air–water interface in the absence and presence of 20 mol% of the antimicrobial peptides UBI (29–41) and UBI-2-APBA. Comparison of (b) maximum area at nonzero surface pressure (A_{max}) and (c) limiting mean molecular area (A_{lim}). (d) Variation in storage (E') and loss (E'') moduli of the monolayer in the absence and presence of the peptides measured at a surface pressure of 25 mN m^{-1}. (e) E' and (f) E'' at a particular frequency of 30 mHz. In the bar graphs, 'WP', 'UBI (29–41)' and 'UBI-2-APBA)' represent 'without peptide' and with respective peptides. All measurements are performed at 22 °C.

larger A_{lim} observed with UBI-2-APBA suggests a higher presence of the peptide in or around the lipid film.

The biological membranes are dynamic and heterogeneous systems where lateral mobility and in-plane fluctuations of lipid composition contribute to complex viscoelastic behaviour. This mechanical response is critically influenced by the lipid phase state, molecular packing, and incorporation of exogenous agents such as peptides.[27,28] In the presence of UBI (29–41)

Table 1 Various parameters of lipid monolayers in the absence and presence of peptides. A_{max}: mean molecular area at the onset of non-zero surface pressure, A_{lim}: estimated area per molecule in the most tightly packed state, determined by extrapolating the linear portion of the isotherm to zero surface pressure, E_{CM}: compressional modulus, which can be calculated from the isotherm data using the equation, $E_{CM} = -A\left(\frac{\partial \pi}{\partial A}\right)_T$. E': storage modulus, quantifies the elastic (energy-storing) and E'': loss modulus represents the viscous (energy-dissipation)

Compositions	A_{max} (Å^2)	A_{lim} (Å^2)	E_{CM} at 25 mN m^{-1} (mN m^{-1})	E' at 30 mHz (mHz)	E'' at 30 mHz (mHz)
Lys PG	183.47 ± 0.85	141.75 ± 0.57	79.61 ± 0.45	24.94 ± 0.16	9.75 ± 0.64
Lys PG + 20 mol% UBI (29–41)	187.29 ± 1.63	146.54 ± 0.90	79.96 ± 0.30	25.78 ± 0.14	11.56 ± 0.48
Lys PG + 20 mol% UBI-2-APBA	209.38 ± 1.33	155.62 ± 0.62	77.79 ± 0.51	29.92 ± 1.50	12.64 ± 0.75
DSEPC	162.12 ± 0.93	89.84 ± 0.66	71.17 ± 1.13	20.64 ± 0.40	8.82 ± 0.63
DSEPC + 20 mol% UBI (29–41)	163.27 ± 0.69	84.9 ± 0.99	82.56 ± 1.09	19.39 ± 0.81	8.01 ± 0.50
DSEPC + 20 mol% UBI-2-APBA	189.27 ± 0.61	108.14 ± 0.86	69.20 ± 0.91	13.02 ± 0.20	3.51 ± 0.70
DSPE	55.36 ± 0.31	36.44 ± 0.35	210.50 ± 1.80	51.70 ± 0.20	22.29 ± 0.60
DSPE + 20 mol% UBI (29–41)	64.92 ± 0.35	50.99 ± 0.40	109.12 ± 1.99	42.80 ± 1.01	14.82 ± 1.06
DSPE + 20 mol% UBI-2-APBA	64.48 ± 0.36	52.04 ± 0.33	118.17 ± 1.96	41.42 ± 0.54	19.46 ± 0.80

and UBI-2-APBA in the lipid film, the in-plane storage modulus (E') and loss modulus (E'') were quantified at a surface pressure of 25 mN m^{-1}, corresponding to the LC phase. Throughout the experiment, the strain amplitude was controlled by oscillating the barrier to 0.5% of the total film area, ensuring that the measurements remained close to the linear viscoelastic regime. Higher strain amplitude causes strong non-linearity which can be visualized from the presence of higher harmonics in the Fourier transform analysis of the pressure response. Such an analysis has been provided in Section S3 of the SI. As shown in Fig. 2(d), across the entire frequency range (10–100 mHz), the storage modulus (E') remains consistently higher than the loss modulus (E'') for all samples, indicating that the Lys PG monolayer exhibits predominantly elastic behaviour. Upon incorporation of antimicrobial peptides UBI (29–41) and UBI-2-APBA, differential effects were observed. In 20 mol% UBI (29–41), there is a modest increase in both E' and E'', suggesting a weak perturbation in the viscoelastic nature of the lipid film. This observation is quite consistent with the surface pressure–area isotherm showing minimal changes in the molecular area, supporting the lack of strong binding or insertion of the peptide to the lipid. In stark contrast, the addition of UBI-2-APBA results in a substantial increase in both E' and E'', signifying a marked enhancement in the film's viscoelasticity. Therefore, the modified peptide is much more efficient to disrupt the self-assembly of the lipid layer. At a particular frequency of 30 mHz, the observation is demonstrated in Fig. 2(e) and (f). The π–A isotherm data showing an increase in the mean molecular area suggests two possibilities: the peptides may adsorb to the lipid head groups to reorient them to occupy more area, or the peptides may insert themselves into the lipid film to occupy physical space. Note that only the number of lipids is considered when calculating the mean molecular area of lipids in the presence of peptides. In the first case, the film would be easily compressible, providing a reduction in E' and E''. The second case will enhance the value of these parameters. As mentioned earlier, this enhancement is attributed to strong interactions between the 2-APBA moiety and the Lys PG headgroups, likely through the formation of an iminoboronate linkage. Such interactions not only increase the film's resistance to deformation (higher E') but also amplify energy dissipation during molecular rearrangements (higher E''). The frequency-dependent modulation of the viscoelastic properties has been reported earlier in phosphoglycerol-based lipid films, where both the acyl chain and lipid phase state critically influence the mechanical response.[22] The shorter lipid chains exhibit minimal frequency dependence, whereas longer-chain lipids show stiffening or softening depending on the presence of additives in the film. These observations highlight the interplay between lipid ordering, electrostatic interactions, and molecular disruption.

3.2. Less amine group leads to weaker affinity of the peptide to cationic lipids

To determine whether the modified peptide UBI-2-APBA exhibits specificity for the bacterial phospholipid Lys-PG or if it can also interact with any other positively charged lipids, we quantified the affinity of the peptides to a monolayer composed of cationic DSEPC as shown in Fig. 3(a). The π–A isotherm of the pure lipid is consistent with previous reports,[29] exhibiting an A_{max} value of 162.1 Å^2 (Table 1) with a collapse pressure of 46 mN m^{-1}. This lipid exhibits a higher A_{max} than other saturated zwitterionic lipids, such as DSPC and DSPE, due to electrostatic repulsion among the cationic headgroups and the steric repulsion among the long hydrocarbon chains.[25] The A_{lim} value is found to be 89.8 Å^2, as shown in Fig. 3(c). The addition of UBI (29–41) results in a minimal change in A_{max}, indicating almost negligible interaction (Fig. 3(b)). Similarly, A_{lim} has a subtle decrease in the value. In contrast, in the presence of UBI-2-APBA, A_{max} increases to 189.3 Å^2, indicating enhanced interactions as shown in Fig. 3(b). Also, A_{lim} increases to 109.8 Å^2 (Fig. 3(c)).[30] This substantial expansion suggests that UBI-2-APBA perturbs the DSEPC monolayer significantly compared to UBI (29–41). The oscillatory viscoelastic measurements for the monolayer formed by DSEPC in the absence and presence of peptides are shown in Fig. 3(d). The monolayer is elastic in nature as E' is greater than E'' for all the cases. The addition of UBI (29–41) makes no change in the viscoelastic parameters. However, a prominent drop in the parameters is observed for the UBI-2-APBA molecules. Fig. 3(e) and (f) show the trend for E' and E'', respectively, in the DSEPC monolayer in the presence of UBI (29–41) and UBI-2-APBA at a particular frequency of 30 mHz. It is interesting to observe that the modified peptide causes a decrease in the values of E' and E'' for DSEPC, which is opposite to the observations for Lys PG lipids. For this DSEPC lipid, the peptides seem to be adsorbed to the head group without inserting themselves well into the lipid film. It is to be noted that each Lys PG contains two amine groups, while a DSEPC has only one. Therefore, the Lys PG will be more effective in assembling a higher number of peptides near the lipid film (see AFM images in Section 3.6), which may cause some of the peptides to insert into the lipid film. As mentioned earlier, the inserted peptides may cause the molecular film to be more rigid.

It is conclusive that the cationic peptides, such as UBI (29–41), are unsuitable to target cell membranes enriched with cationic lipids. As many Gram-positive bacteria have cationic lipids, such as Lys PG, in their cellular membrane, the conventional cationic AMPs are not helpful. However, the modified AMP, such as UBI-2-APBA, even though cationic in nature, can interact with the bacterial membrane because of the formation of a covalent bond between the nitrogen of an imine of the lipid and the boron atom in the peptide. This well-designed peptide with a specificity for amine-bearing lipids is critical for its selective membrane-targeting function.

3.3. Similar affinity of modified and unmodified peptides to zwitterionic lipids

To further investigate the lipid affinity of UBI (29–41) and UBI-2-APBA, the study has been extended to zwitterionic lipid, DSPE. It possesses one amine group with no net charge but a permanent dipole moment. This lipid was selected to examine

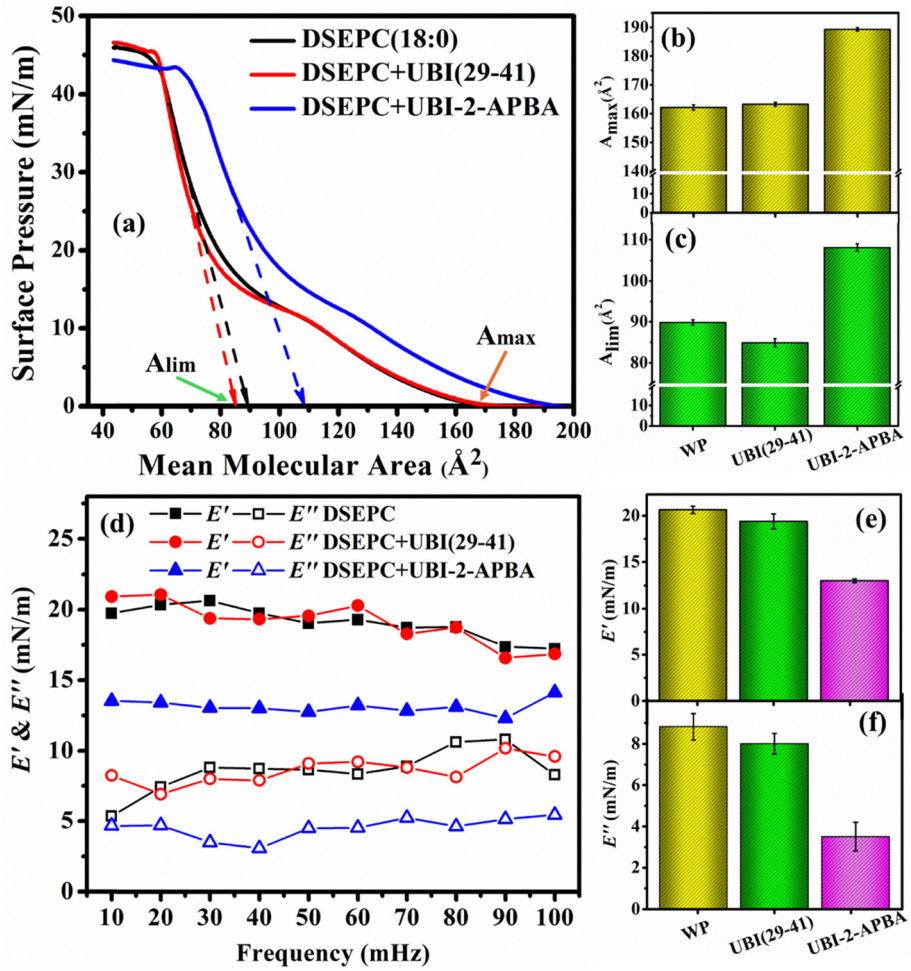

Fig. 3 (a) Surface pressure (π)–area (A) isotherms of the DSEPC monolayer at the air–water interface in the absence and presence of 20 mol% of the antimicrobial peptides UBI (29–41) and UBI-2-APBA. Comparison of (b) maximum area at nonzero surface pressure (A_{max}) and (c) limiting mean molecular area (A_{lim}). (d) Variation in storage (E') and loss (E'') moduli of the monolayer in the absence and presence of the peptides measured at a surface pressure of 25 mN m^{-1}. (e) E' and (f) E'' at a particular frequency of 30 mHz. In the bar graphs, 'WP', 'UBI (29–41)' and 'UBI-2-APBA' represent 'without peptide' and with respective peptides. All measurements are performed at 22 °C.

whether these peptides are equally interactive, like other lipids having an amine group in their head region. Furthermore, the phosphoethanolamines, such as DSPE, are known to form more tightly packed, hydrogen-bonded monolayers compared to phosphatidylcholines, offering a stringent test of the ability of the peptides to perturb densely packed zwitterionic lipid matrices. The π–*A* isotherms of pure DSPE monolayers show the expected behaviour of densely packed films with the A_{max} found to be 55.4 Å^2 (Fig. 4(a)), consistent with previously reported data.[31] Upon incorporation of 20 mol% UBI (29–41), the DSPE monolayer exhibited a measurable shift in A_{max} towards higher values. The value increases to 64.9 Å^2 as shown in Fig. 4(b). A corresponding modest expansion in the A_{lim} was also observed (Fig. 4(c)). There was no electrostatic repulsion between the cationic peptide and the zwitterionic lipid, so the peptide UBI (29–41) may help target a bacterial membrane with such lipids. Similarly, the incorporation of 20 mol% UBI-2-APBA induces shifts in the A_{max} and A_{lim} for the DSPE monolayer comparable to those observed with UBI (29–41). This observation indicates that introducing the 2-APBA moiety does not substantially enhance peptide interaction with a zwitterionic lipid. Instead, both peptides behave similarly in the absence of electrostatic repulsion. Therefore, UBI-2-APBA is particularly relevant to target bacterial membranes with cationic lipid environments.

In Fig. 4(d), the value for E' is observed to be higher compared to E'', which is like other lipids discussed above. The addition of UBI (29–41) to DSPE reduces the viscoelastic nature of the film slightly because of the weak adsorption of the peptide to the lipid film. The effect is stronger in the presence of UBI-2-APBA. Fig. 4(e) and (f) show the trend for E' and E'' respectively for the monolayer in the presence of these peptides at a particular frequency of 30 mHz. It is worth discussing that the values of E' and E'' for the DSPE lipid are much higher compared to the lipids Lys PG and DSEPC indicating a stiffer lipid layer. At this frequency of 30 mHz, the respective values of E' and E'' are 41 mN m^{-1} and 19 mN m^{-1} for the DSPE. The values drop to 30 mN m^{-1} and 12.8 mN m^{-1} for the Lys PG and 12.6 mN m^{-1} and 3.7 mN m^{-1} for DSEPC, respectively.

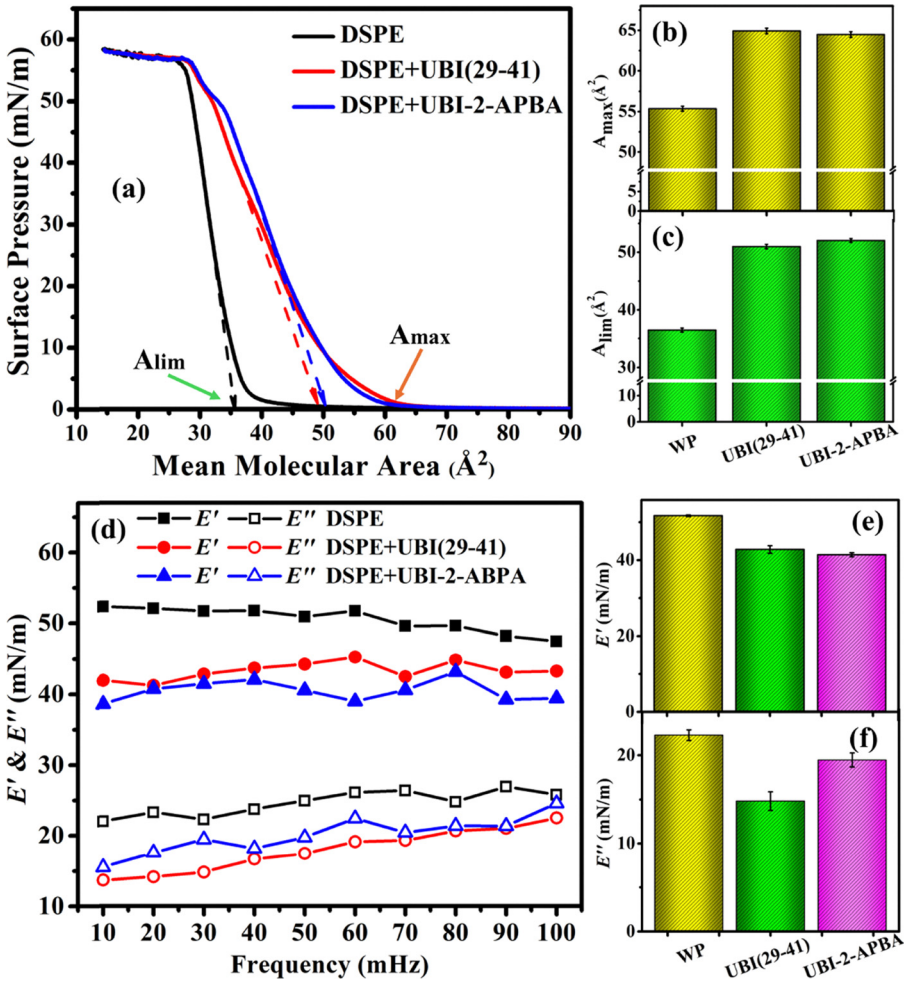

Fig. 4 (a) Surface pressure (π)–area (A) isotherms of the DSPE monolayer at the air–water interface in the absence and presence of 20 mol% of the antimicrobial peptides UBI (29–41) and UBI-2-APBA. Comparison of (b) maximum area at nonzero surface pressure (A_{max}) and (c) limiting mean molecular area (A_{lim}). (d) Variation in storage (E') and loss (E'') moduli of the monolayer in the absence and presence of the peptides measured at a surface pressure of 25 mN m^{-1}. (e) E' and (f) E'' at a particular frequency of 30 mHz. In the bar graphs, 'WP', 'UBI (29–41)' and 'UBI-2-APBA' represent 'without peptide' and with the respective peptides. All measurements are performed at 22 °C.

These observations can be explained in terms of the close and compact packing of the DSPE lipids in the monolayer compared to the others.

The in-plane static elasticity of all the lipid films discussed in the above sections can be calculated from the slope of the isotherms using the equation, $E_{CM} = -A\left(\frac{\partial \pi}{\partial A}\right)_T$ where π is the surface pressure and A is the molecular area at a temperature T. Fig. S13 shows the elasticity curves plotted against surface pressure. For the Lys PG, dynamic elasticity, which was quantified at a surface pressure of 25 mN m^{-1}, shows a slight increase in its value on the addition of the peptides (Fig. 2(d)). The static elasticity for this lipid remains almost invariant (Fig. S13(a)) at the same pressure. For the DSEPC lipid, both the dynamic and the static elasticity curves follow a similar trend. As shown in S13(c), a considerable drop in the static elasticity is observed for the DSPE lipid in the presence of both the peptides, which was exactly the case when the dynamic elasticity was quantified for this lipid (Fig. 4(d)). The quantitative values of this static and dynamic elasticity may not be the same as the values are measured as a function of different experimental variables with differences in their sensitivity; however, the qualitative changes follow a similar trend. Table 1 summarizes the static elasticity E_{CM} and the dynamics storage modulus (E') for lipids in the presence and absence of the peptides.

3.4. Peptide to modify the surface potential of cationic lipids

Since the boronated ubiquicidin peptide UBI-2-APBA is specifically relevant for the cationic lipid Lys PG, the effect of this peptide, along with the non-boronated one, has been quantified in terms of the surface electrostatic potential of the lipid monolayer. In this study, surface potential (ΔV)–area (A) isotherms were measured concurrently alongside π–A isotherms, using identical chemical component concentrations. The surface potential (ΔV), representing the potential difference between a pure water surface and a monolayer-covered surface, is influenced by the molecular composition in the film at the interface with their packing density and molecular orientation.

Each potential curve is an average of at least three independent measurements keeping the instrumental set up, such as gap between the electrodes, distance of the top electrode from the water surface *etc.*, identical. As shown in Fig. 5(a), the cationic lipid shows a positive value of the potential overall in the mean molecular area of the lipid because of two positively charged amine groups on each head of Lys PG. The enhanced value of the potential on decreasing the mean molecular area is understood from the higher density of the lipids at the interface.

As shown in Fig. 5(b), a decrease in surface potential was observed in the presence of 20 mol% of unmodified UBI (29–41) in the Lys PG film. Even though these peptides may not insert themselves into the lipid film, their presence around the film may influence the number density of the lipids and their orientation at the interface, exhibiting a decrease in potential. The addition of the modified UBI-2-APBA led to an increase in surface potential, suggesting a different mode of interaction. This implies that the modified peptide can overcome electrostatic barriers, facilitating a favourable insertion into the lipid monolayer, causing an overall enhanced positive charge density at the interface.[32] Such a possibility of insertion is discussed earlier in explaining the dilation rheology data shown in Fig. 2(d). These results highlight the crucial role of chemical modifications in mediating lipid interface interactions, especially in electrostatically unfavourable environments. Our findings are in line with previous studies on other antimicrobial peptides, such as LL-37 and its analogues, in which variants of LL-37 with increased positive charge demonstrated enhanced interactions with lipid monolayers, as evidenced by changes in surface pressure and potential measurements.[32,33]

3.5. Variable kinetics of assembly of peptides around cationic lipids

The extent of affinity of a macromolecule to a specific lipid can be quantified by measuring the change in surface pressure of the lipid film floating at the air–water interface after injecting the macromolecule into the subphase of the film (see inset of Fig. 6). Here, the monolayer of Lys PG was equilibrated to a surface pressure of $\sim$20 mN m^{-1}, then the peptides UBI (29–41) and UBI-2-APBA were injected in the subphase. The surface pressure was monitored as a function of time. Over time, the peptides diffuse to the lipid layer and self-assembled around it which causes the surface pressure to increase. The percentage change in this pressure for the monolayer of pristine lipid and the monolayers in the presence of these two peptides is shown in Fig. S14 (Section S5 in SI). The effects of the peptides relative to the pristine lipid are presented in Fig. 6. This is obtained from the data plotted in Fig. S14 after subtracting the background pressure increment in the pristine lipid. The injected peptides could not generate any surface pressure in the absence of the lipid layer at the air–water interface, which is expected as they themselves are not surface active (see isotherm in Fig. 2(a)). As evident in Fig. 6, the increase in surface pressure is faster for the UBI-2-APBA compared to the UBI (29–41). Furthermore, the saturated pressure is considerably higher for the modified peptide. Therefore, it can be unambiguously stated that the modified peptide UBI-2-APBA has a better affinity to the Lys PG.

3.6. Visualizing assembled peptides around cationic lipids

Though the observations described in the above sections suggested that the modified peptide UBI-2-APBA has a preferential affinity to the Lys PG compared to the UBI (29–41), the data did not present a direct visualization of the conclusions. Therefore, the lipid monolayers in the absence and presence of these peptides were transferred on a Si-substrate to investigate the morphologies through AFM imaging (Fig. 7). While the pristine Lys PG monolayer shows a relatively smooth and uniform surface, the monolayer with 20 mol% UBI (29–41) displays a few discrete structures with an average height of 9.2 $\pm$ 2.38 nm. The structures suggest the presence of the peptides at the lipid interface, indicating the UBI (29–41) to interact with cationic Lys PG, but the extent of their assembly around the lipid layer remains relatively modest. In contrast, the addition of 20 mol% UBI-2-APBA results in pronounced morphological changes showing numerous large structures with an average

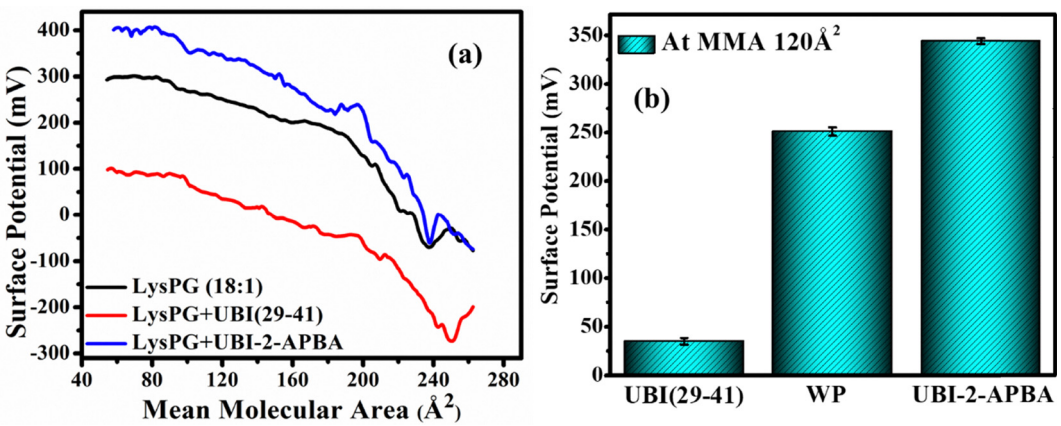

Fig. 5 (a) Surface potential (ΔV)–area (A) isotherms of lipid Lys PG monolayers formed at the air–water interface without peptide (WP) and in the presence of 20 mol% of the antimicrobial peptides UBI (29–41) and UBI-2-APBA, and (b) surface potential value at a particular mean molecular area (MMA) of 120 Å^2.

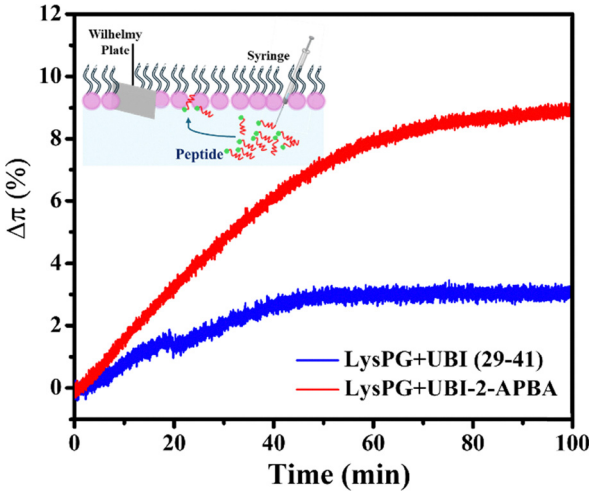

Fig. 6 Percentage change of surface pressure (π) of the Lys PG monolayer with time due to injection of UBI (29–41) (blue curve) and UBI-2-APBA (red curve) peptides in the subphase at an initial surface pressure of ~20 mN m^{-1}. The change is plotted relative to the change observed in pristine Lys PG. Inset: Schematic of the experiment showing the injected peptides diffusing to the lipid monolayer.

height of 24.1 ± 5.10 nm. As evident from Fig. 7(b) and (c), the in-plane size of these structures is larger for UBI-2-APBA compared to that of the UBI (29–41). These prominent surface heterogeneities suggest that UBI-2-APBA interacts strongly with Lys PG as predicted from enhanced perturbations detected in the isotherm, in-plane rheology, and the marked variations in the surface potential.

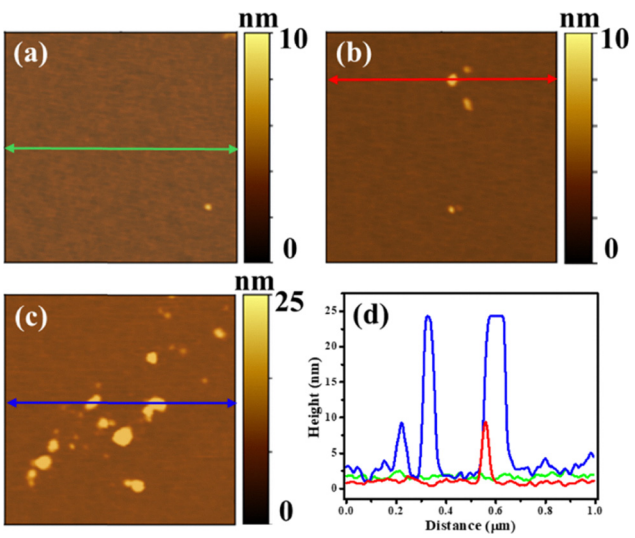

Fig. 7 Atomic force microscopy (AFM) images of (a) pure Lys PG monolayer, and Lys PG monolayer in the presence of (b) 20 mol% UBI (29–41), and (c) 20 mol% UBI-2-APBA. (d) Corresponding height profiles of all three systems following the lines shown in the AFM images. The profiles represent the height from the lipid monolayer surface, not from the underlying Si-substrate. Monolayers were transferred onto silicon substrates using the Langmuir–Blodgett technique at a surface pressure of 30 mN m^{-1}. The AFM topography images have a scan size of 1 × 1 μm^2.

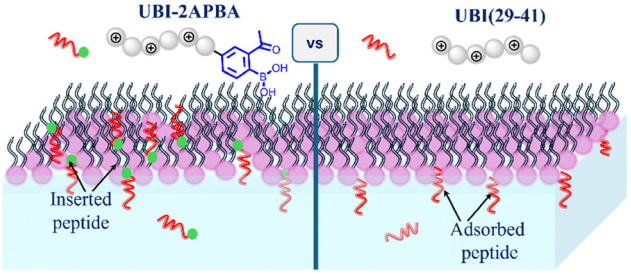

Fig. 8 Schematics of assembly of antimicrobial ubiquicidin peptide UBI (29–41) and boronated ubiquicidin peptide UBI-2-APBA at a monolayer containing cationic lipid Lys-PG formed at the air–water interface. While UBI-2-APBA shows an in-depth penetration into the monolayer, the UBI (29–41) only adsorbs on the layer.

The difference in the assembly of UBI-2-APBA depending on the type of lipid has also been investigated by AFM imaging. As shown in Fig. S15, a higher number of heterogeneous structures are observed near the Lys PG monolayer compared to the monolayers formed by DSEPC and DSPE. As discussed in Section S6 of the SI, the in-plane size and the height of the structures are relatively larger for the Lys PG monolayer.

As discussed earlier,[13] the Lys PG and PE are the major lipids in the bacterial membrane while a mammalian membrane predominantly contains phosphatidylcholine (PC). As observed in the present study, the modified peptide UBI-2-APBA shows affinity to both Lys PG and PE through the formation of covalent linkage with amines. However, because of the absence of the amine group, the peptide may not be active to the PC lipids. Therefore, the host cell may not be affected by the modified peptide. However, a systematic study is required to quantify the effect of this peptide on the major lipids which are present in a host mammalian cell.

The main aim of the present study was to compare the affinity of the modified peptide to the crucial lipids present in antimicrobial resistance bacteria. Hence, the simple system of a lipid monolayer at the air–water interface was utilized, which offers information on peptide–lipid affinity through interfacial phenomena. However, this alone is incapable of presenting the full range of antimicrobial activity of the peptides, as membrane morphology, organization and mechanical stress are crucial factors. Bilayer systems like unilamellar or multilamellar vesicles would be a more sophisticated model system to explore the effect of the peptides on membranes. This is a subject of future studies.

4. Conclusions

This study establishes a distinct hierarchy in the lipid-binding affinities of UBI (29–41) and its boronic acid-functionalized, modified peptide UBI-2-APBA (Fig. 8). The UBI-2-APBA exhibits substantially stronger interactions than UBI (29–41) in cationic environments, owing to its ability to form covalent iminoboronate bonds with primary amine groups present in lipids Lys PG and DSEPC. However, the Lys PG causes the peptide to be inserted into the lipid film, while the DSEPC lipid adsorbs the

peptide into the lipid film. When interacting with zwitterionic lipid DSPE, UBI (29–41) and UBI-2-APBA display similar interaction profiles. The covalent targeting mechanism provides a robust strategy for selective discrimination between bacterial membranes, enhancing the potential of UBI-2-APBA against antibiotic resistant bacteria. This fundamental biophysical analysis may help to develop advanced diagnostics and therapeutics to combat bacterial infections in the near future.

Conflicts of interest

There are no conflicts to declare.

Data availability

The datasets supporting this article have either been included in the article itself or uploaded as part of the supplementary information (SI). Supplementary information is available. See DOI: **https://doi.org/10.1039/d5sm00692a**.

Acknowledgements

All the authors are thankful to the Board of Research in Nuclear Sciences (BRNS), Department of Atomic Energy (DAE), Govt. of India, for the financial support to conduct the research through a project with sanction number 58/14/13/2022-BRNS/37059 and 58/14/12/2022-BRNS/37058. Special thanks go to Dr Jyotsna Bhatt Mitra for useful scientific discussions.

References

1 S. Zheng, *et al.*, Antimicrobial peptide biological activity, delivery systems and clinical translation status and challenges, *J. Transl. Med.*, 2025, **23**(1), 292, DOI: **10.1186/s12967-025-06321-9**.
2 M. Michalik, A. Podbielska-Kubera and A. Dmowska-Koroblewska, Antibiotic resistance of Staphylococcus aureus strains—searching for new antimicrobial agents, *Pharmaceuticals*, 2025, **18**(1), 81.
3 R. E. W. Hancock and A. Patrzykat, Clinical development of cationic antimicrobial peptides: from natural to novel antibiotics, *Curr. Drug Targets:Infect. Disord.*, 2002, **2**(1), 79–83.
4 P. L. Moja and W. H. Organization, Prioritization of pathogens to guide discovery, research and development of new antibiotics for drug resistant bacterial infections, including tuberculosis, 2017, Accessed: Apr. 28, 2025. [Online]. Available: **https://air.unimi.it/handle/2434/533960**.
5 N. A. Church and J. L. McKillip, Antibiotic resistance crisis: challenges and imperatives, *Biologia*, 2021, **76**(5), 1535–1550, DOI: **10.1007/s11756-021-00697-x**.
6 Y. Cai, *et al.*, Self-Assembling Lauroylated Antimicrobial Peptide with Superior Antimicrobial Activity, Stability, and Selectivity, *ACS Appl. Mater. Interfaces*, 2025, **17**(9), 13646–13659, DOI: **10.1021/acsami.4c22552**.
7 P. Thakral, *et al.*, Validation of Radiosynthesis and First in-Human Dosimetry of ^{68}Ga-NOTA-UBI-29-41: A Proof-of-Concept Study, *Cancer Biother. Radiopharm.*, 2025, **40**(2), 104–113, DOI: **10.1089/cbr.2024.0082**.
8 G. C. Schito, The importance of the development of antibiotic resistance in *Staphylococcus aureus*, *Clin. Microbiol. Infect.*, 2006, **12**, 3–8, DOI: **10.1111/j.1469-0691.2006.01343.x**.
9 J. Andrä, T. Goldmann, C. M. Ernst, A. Peschel and T. Gutsmann, Multiple peptide resistance factor (MprF)-mediated resistance of Staphylococcus aureus against antimicrobial peptides coincides with a modulated peptide interaction with artificial membranes comprising lysyl-phosphatidylglycerol, *J. Biol. Chem.*, 2011, **286**(21), 18692–18700.
10 E. Cox, A. Michalak, S. Pagentine, P. Seaton and A. Pokorny, Lysylated phospholipids stabilize models of bacterial lipid bilayers and protect against antimicrobial peptides, *Biochim. Biophys. Acta, Biomembr.*, 2014, **1838**(9), 2198–2204.
11 M. Tollin, P. Bergman, T. Svenberg, H. Jörnvall, G. H. Gudmundsson and B. Agerberth, Antimicrobial peptides in the first line defence of human colon mucosa, *Peptides*, 2003, **24**(4), 523–530.
12 C. M. C. Andrés, J. M. Pérez de la Lastra, E. B. Munguira, C. A. Juan and E. Pérez-Lebeña, Selenium Nanoparticles in Critical Illness—Anti-Inflammatory and Antioxidant Effects, *Dietetics*, 2025, **4**(1), 6.
13 A. Bandyopadhyay, K. A. McCarthy, M. A. Kelly and J. Gao, Targeting bacteria via iminoboronate chemistry of amine-presenting lipids, *Nat. Commun.*, 2015, **6**(1), 6561.
14 J. B. Mitra, S. Chatterjee, A. Kumar, A. Bandyopadhyay and A. Mukherjee, Integrating a covalent probe with ubiquicidin fragment enables effective bacterial infection imaging, *RSC Med. Chem.*, 2022, **13**(10), 1239–1245.
15 J. Bhatt Mitra, *et al.*, Expanding a peptide-covalent probe hybrid for PET imaging of *S. aureus* driven focal infections, *EJNMMI Radiopharm. Chem.*, 2024, **9**(1), 25.
16 MICAD Research Team, 99mTc-Ubiquicidin29-41, Mol. Imaging Contrast Agent Database MICADInternet, 2007.
17 B. K. Das, *et al.*, Harnessing a bis-electrophilic boronic acid lynchpin for azaborolo thiazolidine (ABT) grafting in cyclic peptides, *Chem. Sci.*, 2024, **15**(34), 13688–13698.
18 P. Hitaishi, P. Mandal and S. K. Ghosh, Partitioning of a Hybrid Lipid in Domains of Saturated and Unsaturated Lipids in a Model Cellular Membrane, *ACS Omega*, 2021, **6**(50), 34546–34554.
19 R. Miller, J. K. Ferri, A. Javadi, J. Krägel, N. Mucic and R. Wüstneck, Rheology of interfacial layers, *Colloid Polym. Sci.*, 2010, **288**, 937–950.
20 R. Miller and L. Liggieri, *Interfacial rheology*, CRC Press, 2009, vol. 1, Accessed: May 01, 2025. [Online]. Available: **https://books.google.com/books?hl=en&lr=&id=pT9pNObvRD8C&oi=fnd&pg=PP1&dq=Miller,+R.%3B+Liggieri,+L.+Interfacial+Rheology%3B+CRC+Press,+2009%3B+Vol.+1&ots=_gsi8317nM&sig=5qDpyL4-3o59KwO4c8LA_W_XgHyM**.
21 A. J. Mendoza, *et al.*, Particle laden fluid interfaces: Dynamics and interfacial rheology, *Adv. Colloid Interface Sci.*, 2014, **206**, 303–319.

22 P. Hitaishi, A. Seth, S. Mitra and S. K. Ghosh, Thermodynamics and in-plane viscoelasticity of anionic phospholipid membranes modulated by an ionic liquid, *Pharm. Res.*, 2022, **39**(10), 2447–2458.
23 B. Bera, Silicon wafer cleaning: a fundamental and critical step in semiconductor fabrication process, *Int. J. Appl. Nanotechnol.*, 2019, **5**(1), 8–13.
24 A. P. Girard-Egrot and L. J. Blum, Langmuir-Blodgett Technique for Synthesis of Biomimetic Lipid Membranes, in *Nanobiotechnology of Biomimetic Membranes*, ed. D. K. Martin, in Fundamental Biomedical Technologies, Springer US, Boston, MA, 2007, vol. 1, pp. 23–74, DOI: 10.1007/0-387-37740-9_2.
25 S. Raghav, P. Hitaishi, R. P. Giri, A. Mukherjee, V. K. Sharma and S. K. Ghosh, Selective assembly and insertion of ubiquicidin antimicrobial peptide in lipid monolayers, *J. Mater. Chem. B*, 2024, **12**(45), 11731–11745, DOI: 10.1039/D4TB01487A.
26 J. Pérez-Gil and K. M. Keough, Interfacial properties of surfactant proteins, *Biochim. Biophys. Acta, Mol. Basis Dis.*, 1998, **1408**(2–3), 203–217.
27 P. Hitaishi, *et al.*, Cholesterol-Controlled Interaction of Ionic Liquids with Model Cellular Membranes, *Langmuir*, 2023, **39**(27), 9396–9405, DOI: 10.1021/acs.langmuir.3c00883.
28 D. Kaushik, P. Hitaishi, A. Kumar, D. Sen, S. M. Kamil and S. K. Ghosh, Modulating a model membrane of sphingomyelin by a tricyclic antidepressant drug, *Chem. Phys. Lipids*, 2024, **263**, 105419.
29 A. Seth, P. Mandal, P. Hitaishi, R. P. Giri, B. M. Murphy and S. K. Ghosh, Assembly of graphene oxide vs. reduced graphene oxide in a phospholipid monolayer at air–water interfaces, *Phys. Chem. Chem. Phys.*, 2025, **27**(4), 1884–1900, DOI: 10.1039/d4cp02706j.
30 D. Marsh, Lateral pressure profile, spontaneous curvature frustration, and the incorporation and conformation of proteins in membranes, *Biophys. J.*, 2007, **93**(11), 3884–3899.
31 F. Neville, *et al.*, Lipid Headgroup Discrimination by Antimicrobial Peptide LL-37: Insight into Mechanism of Action, *Biophys. J.*, 2006, **90**(4), 1275–1287, DOI: 10.1529/biophysj.105.067595.
32 T. Kundlacz, C. Schwieger and C. Schmidt, Effects of Surface Charge of Amphiphilic Peptides on Peptide–Lipid Interactions in the Gas Phase and in Solution, *Anal. Chem.*, 2025, **97**(10), 5808–5817, DOI: 10.1021/acs.analchem.5c00283.
33 A. Bonfanti, J. L. Kaplan, G. Charras and A. Kabla, Fractional viscoelastic models for power-law materials, *Soft Matter*, 2020, **16**(26), 6002–6020.